



Contents lists available at ScienceDirect

Analytica Chimica Acta

journal homepage: [www.elsevier.com/locate/aca](http://www.elsevier.com/locate/aca)



## New method for sintering silica frits for capillary microcolumns

Sonia Keunchkarian<sup>a</sup>, Pablo J. Lebed<sup>a</sup>, Brenda B. Sliz<sup>a</sup>, Cecilia B. Castells<sup>a,b</sup>,  
Leonardo G. Gagliardi<sup>a,b,\*</sup>

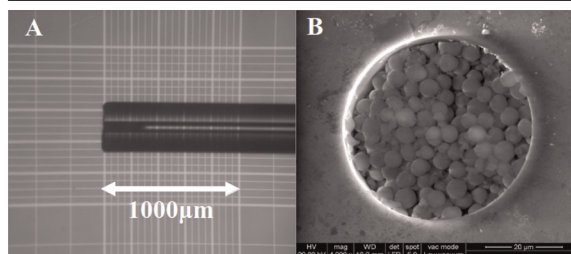
<sup>a</sup> Laboratorio de Investigación y Desarrollo de Métodos Analíticos (LIDMA), Universidad Nacional de La Plata, Calle 47 y 115 (1900), La Plata, Buenos Aires, Argentina

<sup>b</sup> Centro de Investigación y Desarrollo en Tecnología de Pinturas (CIDEPIINT-CIC-CONICET), Av. 52 y 120 (1900), La Plata, Buenos Aires, Argentina

### HIGHLIGHTS

- We propose and optimize a new procedure to form silica end frits in capillary columns.
- The method is based on thermal sintering of particles using axial transfer of heat.
- The method is robust, reproducible and save the polyimide coatings.
- The obtained frits are short, permeable, resistant, efficient and do not form bubbles.

### GRAPHICAL ABSTRACT



### ARTICLE INFO

#### Article history:

Received 21 December 2013  
Received in revised form 12 February 2014  
Accepted 16 February 2014  
Available online xxx

#### Keywords:

Electrochromatography  
Capillary microcolumns  
Sintered silica frits

### ABSTRACT

One of the main steps in the manufacture of robust and efficient packed capillary microcolumns for electro- and capillary chromatography is the generation of porous devices to retain the packed beds. Frits based on sintered silica particles have been found to give the best results in terms of mechanical resistance and efficiency. The conventional procedure to produce these kinds of frits consists in a radial heating of the packed material with either a flame or an electrical resistance, but the frits thus obtained have many drawbacks as a result of the procedure rather than the silica *per se* as the base material. In the present work we investigated a new approach to produce silica-based retaining devices involving the frontal exposure of a short silica-particle bed packed at the end of a capillary tube. The capillary is radially insulated and frontally exposed to the heat of a muffle oven, generating a transfer of heat that is not radial but rather throughout the capillary axis. This procedure resulted in substantial advantages: an improved radial homogeneity, a protection of the external polyimide, and a generation of extremely short (400–600  $\mu\text{m}$ ) frits that were highly permeable and avoided bubble formation.

© 2014 Published by Elsevier B.V.

### 1. Introduction

Capillary electrochromatography (CEC) combines the advantages of the wide diversity of stationary phases available for HPLC with the excellent efficiencies usually achievable in electrodriven techniques. These higher efficiencies are based on: (i) the planar

electroosmotic-flow (EOF) profiles, with their characteristic dramatically reduced band dispersions, and (ii) the advantage that reasonable flows can be established with either columns as long as 1 m or even longer, or those based on sub-2  $\mu\text{m}$  particles. Since the early years of CEC, efficiencies as high as 200,000 plates/m have been reported [1–3]. Comparative analysis of the same samples on identical packed capillary columns have shown that more than two fold greater numbers of theoretical plates could be obtained on electrodriven runs over the pressure-driven chromatographies [4].

\* Corresponding author. Fax: +54 2214226947.

E-mail address: [leogagliardi@quimica.unlp.edu.ar](mailto:leogagliardi@quimica.unlp.edu.ar) (L. G. Gagliardi).

A critical subject with respect to the CEC techniques – and also one of the limiting aspects in their adoption for use in routine analysis – is a poor reproducibility. Different causes contribute to this problem. Whereas variability exists in the EOF – a characteristic not dealt with in the present work – this technique is hampered by a lack of reproducible and robust methods to obtain the appropriate capillary columns. The manufacture of a capillary column consists in a sequence of steps, and each of them deserves a specific study in an effort to gain an optimization of the variables that affect efficiency and reproducibility. In most of the studies devoted to the production of CEC columns, the researchers concern themselves with an advance in a particular aspect, but the results are usually expressed in terms of the efficiency achieved in the overall CEC runs. This approach evaluates the whole manufacturing process with little emphasis on the improvement in the individual steps involved.

One of the known key steps in the reproducible production of efficient capillary microcolumns is the generation of the porous device to retain the packing material. Colon et al. [1] stated that this endpiece, the so-called “frit”, is the “Achilles heel” in the fabrication of columns for CEC. Different procedures have been described to form frits, but the more widely used method – the one proposed by Smith et al. [2] – consists in the heating a few millimeters of the capillary tube packed entirely with a bed of silica-particle, followed by a removal of the not sintered loose particles. This approach has some recognized disadvantages [3], – namely: (1) a difficulty in generating the frit reliably and reproducibly, (2) an alteration in the characteristics of the stationary phase (if any) within the frit itself, (3) a difficulty in controlling the permeability of the frit, (4) a weakness in the capillary wall where the frit is located, (5) a band broadening caused by the presence of the frit, and (6) bubble formation and adsorption of polar analytes onto the frit. Despite these drawbacks, this particular sintering method is still used and nowadays even more widely so. In favor of the use of sintered silica frits, Piraino and Dorsey demonstrated that those frits provide significantly better qualities in terms of band dispersions over other porous retaining devices [4].

After this last review there have been just few reports aiming to solve specifically the drawbacks of the inorganic silica, seizing its advantages. Most of the research groups turned their work lines toward the use of other kind of materials such as polymers, which are more easy to use, but also these are physically and chemically less compatible with the capillary wall. Zhang et al. proposed to insert a single high porosity silica particle in the capillary tube and, then, sintering it by external heating [5]. Tan et al. proposed to use a stainless-steel tube as insulating material to restrict the zone heated by a burning flame, obtaining extremely short end-frits on pulled tips outlets of LC–ESI–MS capillary microcolumns LCESIMS [6]. The method hereby proposed involves an axial transfer of heat from a muffle furnace over the end of a silica-packed bed. Certain properties would be expected to be improved with frits produced in this way: (i) radial homogeneity, (ii) much shorter lengths than formed by radial heating, and (iii) frit generation at the precise tip of the capillary tubes.

The use of a muffle oven could provide a more precise control of the temperature along with the possibility of removing the capillary tube immediately, thus allowing a more accurate control of the exposure times with a consequent improvement in reproducibility.

The sintering of a bed of silica particles packed at the end of the capillary tube combined with the use of an insulation for the external polyimide would be likely to provide a more controlled heat penetration and would be expected to generate shorter frits for shorter exposures of the silica particles to the sintering heat.

Shorter frits might, for their part, produce both a lower pressure drop and less band broadening. Another promising advantage of the shorter frits is related to bubble formation. This problem was

observed in the early years of CEC, and many authors reported different explanations for the cause. Accordingly, Carney et al. [7] conducted a specific study of bubble formation and demonstrated that even at high voltages and on uncoated silica frits the phenomenon no longer occurred if the frits were sufficiently short. Finally, since the new method proposed here involves the generation of frits at the end of the capillary tube along with the use of an external insulation, the polyimide coating should be protected to some extent. Even if that layer was completely removed, commercial instruments use prepunchers or open vials and then the capillary tips are immersed free and without making contact with the sample vials or the rubber caps.

## 2. Experimental

### 2.1. Instrumentation

Heat treatments were done in a standard muffle furnace. Frit lengths were measured by means of an Arcano ST ( $\times 20/\times 60$ ) binocular magnifier with reference to the scale of a Neubauer counting chamber (Marienfeld GmbH & Co.). A FEI Quanta 200 scanning electron microscope (FEI, Tokio, Japan) equipped with an Edax energy-dispersive X-ray spectroscopy (EDS) was used to study the sintered materials and an Agilent 1100 HPLC (Waldbron, Germany) pump employed for testing the frit resistance to pressure. The capillary-electrophoresis instruments used were an HPCE model G1600 AX (Waldbron, Germany) and a Lumex Capel 105M (Saint Petersburg, Russia).

### 2.2. Reagents and materials

The silica particles employed were Nucleosil of 5  $\mu\text{m}$  and 120  $\text{\AA}$  average pore size and 10  $\mu\text{m}$  and 85  $\text{\AA}$  from Macherey-Nagel GmbH & Co. Fused capillary tubes (50  $\mu\text{m}$  i.d., 365  $\mu\text{m}$  o.d.) were purchased from Microquartz (Munich, Germany). The solvents used were ultrapure water obtained from a MilliQ Simplicity 185 Millipore, and the methanol HPLC grade from Merck. Other chemical reagents, such as benzyl alcohol, borax, hydrochloric acid (37%, v/v) and sodium hydroxide were of analytical grade.

All necessary cautions were taken into account for solvents and reagent handling. Chemical waste was disposed for a proper residual treatment.

### 2.3. Procedures

Two different methods to introduce the particles into the capillary tubes were evaluated, one based on the use of dry particles and the other on the use of a paste of particles: with water.

#### 2.3.1. Wet-particle packing method (WPM)

A paste was prepared with a simple mixture of silica particles and deionized water. The consistency of this paste is critical; and, in agreement with the recommendation of Boughtflower [8] the optimal quantity of water is that which enables the paste to just stick to the side of a glass vial when pressed with a spatula – i.e., almost dry. In the present preparations, this consistency was attained by mixing 5 mg of 5- $\mu\text{m}$  silica particles with 250  $\mu\text{L}$  of deionized water. This paste was then introduced into the capillary tube by tapping the tube into the slurry repeatedly until more than the length needed was filled – e.g., more than 2 mm. Finally, the solvent is evaporated by heating for 30 min at 105  $^{\circ}\text{C}$  in a still-air oven (without forced convection) followed by another 30 min at 180  $^{\circ}\text{C}$ .

#### 2.3.2. Dry-particle packing method (DPM)

The silica particles were dried for 3 h at 180  $^{\circ}\text{C}$ . After cooling in a desiccator, 1 mg of particles was placed in 1.5-mL plastic vials. In a

step similar to that described for the WPM above, the introduction of particles was performed by tapping the capillary into the bed of dried particles repeatedly. Capillary lengths in excess of 2 mm were packed. In general the number of taps required is between 30 and 40. This procedure was practiced with particles either 5  $\mu\text{m}$  or 10  $\mu\text{m}$  in size.

### 2.3.3. Sintering

In order to avoid radial heating and to expose the capillary tubes to only an axial transfer of heat, the capillaries filled with particles were placed inside a 70-mm  $\times$  8-mm – diameter plaster cylinder through a 0.4-mm hole drilled through its entire length. The plaster turns out to be an excellent material for these purposes: the substance is easy to drill, even with a similar silica capillary tube used exclusively as a bit, and resists the high temperatures of the muffle furnace, while providing a good radial insulation of the

capillary walls. The tips of the packed capillary tubes were set exactly at the border of the plaster bar.

In the first experiments the introduction of the plaster-encased capillaries were done as a single step. However, the changes of temperature resulted too drastic for the silica of the capillary tube, producing breaks and holes similar to spots of laser-ablation, over the cleanly-cut surfaces of the capillary tubes. Then, an additional step was introduced which consisted in expose for few seconds at 5 cm away the surface of the plaster bar to the infrared radiation coming out from inside of the muffle oven through the hole in its door. This pre-heating step solved the problem and, then, it was adopted as a part of the standard procedure in all the experiments. Then, the sets capillary-plaster bar were introduced into the muffle furnace through the 10-mm – diameter hole door into the furnace in order to expose 2 cm of the plaster bar to the internal heat (Fig. 1). After the lapse of time determined for each experiment the

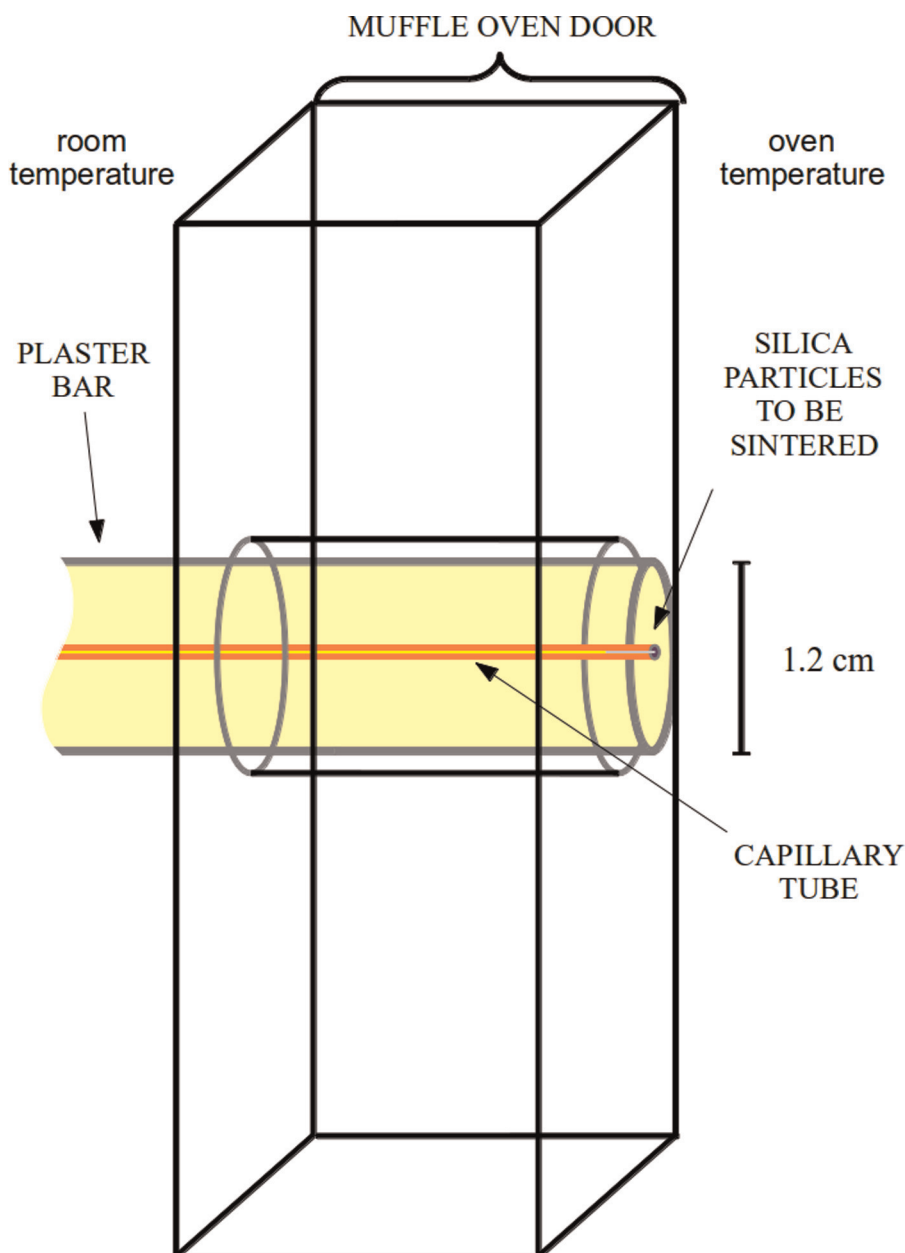


**Fig. 1.** A capillary tube with a silica-particle bed at its tip and placed in an insulating plaster bar, is exposed to the flameless internal heat of the muffle oven after insertion of the bar through a hole in the oven door.

capillaries were rapidly cooled down by removing them from the plaster bar. Finally, after an examination of the bed, the loose particles were removed by a backflushing with methanol, first at low pressure (3 bar) by means of a nitrogen-pressurized vial, then at high pressure with an HPLC pump. This second backflushing was also used to test the frit resistances at the pressures suggested as being sufficient to indicate the ability to withstand a subsequent packing at high pressures (*i.e.*, 55–69 bar) [9].

In order to control the increase in pressure across the frit, a pneumatic buffer was used: the capillaries were connected to an HPLC pump but in our case connecting also, vertically and in parallel to the flow line, an empty stainless-steel tube using a T connector. The air contained in this tube acted as the pneumatic buffer. This device provided a precise control of the pressures. Once the maximum pressure was reached, the pump was stopped and the buffer maintained the flow through the frit for a further length of time.

The use of a split valve instead of the pneumatic buffer was also considered. In both instances the pressure can be fairly well controlled, but the flow rates set in the pump do not correspond to those passing through the frits. Therefore, the drops in pressure and frit permeabilities were determined on a CEC instrument.

#### 2.3.4. Properties of the sintered frits

For each condition the percent success was noted and the morphology, sintered length, permeability, and breaking pressure studied. We considered a “success” in the sintering procedure when the frit remained in place after 15 min of methanol backflushing at 3 bar.

The aspects of the morphology evaluated were: the homogeneity of the sintered material, the presence or absence of voids, and the slopes of the end surfaces. At the same time the total length of the sintered material was measured.

The morphological structure of the frits was studied by scanning electron microscopy (SEM) and an analysis of specific spots carried out with an EDS probe analyzer.

Between 6 and 12 replicates were sintered and evaluated by the above-mentioned procedures under different conditions of exposure time – *i.e.*, 30, 60, and 120 s – and temperature – *i.e.*, 640 °C, 680 °C, 720 °C, and 760 °C.

Frit permeability can be calculated from the elution time of a dead-volume marker (*e.g.*, benzyl alcohol) measured with a 50% (v/v) methanol/water mixture flowing at a constant pressure (1000 mbar) with the capillary kept at 25 °C by a thermostat. The values were obtained upon consideration of the drop in pressure along an empty tube of the same length and *i.d.*

For some of the tested samples the pneumatic buffer was used to determine the breaking pressures. In these instances the pressure was slowly raised, but after a period of rinsing the pressure was gradually increased further up to the breaking point of the frit, when a sudden pressure drop would become recorded by the instrument.

The EOFs were measured on the CE instrument and the values were compared between capillaries with and without frits. For this aim, a 5 mM solution of borax ( $\text{Na}_2\text{B}_4\text{O}_7 \cdot 10\text{H}_2\text{O}$ ;  $I = 10 \text{ mM}$ ) in 10% (v/v) methanol was used as a background electrolyte, and a sample solution of 0.04% (v/v) benzyl alcohol prepared in the same background electrolyte (BGE) was injected. Since the frits produce higher drops of pressure, then, different injection conditions have been used in order to inject similar volumes: in capillaries with frits the injections were done by applying 50 mbar during 10 s, whereas in capillaries without frit these were done by applying 20 mbar during 3 s. The runs were done by triplicate using an inlet voltage of +25 kV (positive).

In order to test the behavior of the frits with respect to the formation of bubbles a capillary tube with a frit of length 550  $\mu\text{m}$

was cut to the shortest possible length for use in the instrument (*e.g.*, total length = 31 cm). With a solution of 50 mM borax in 10% (v/v) methanol as the BGE, a program of voltage was run at either a positive or a negative polarity.

### 3. Results and discussion

#### 3.1. Frit morphology

SEM and magnified imaging of the frits generated by the different methods for introducing particles provided instructive information. Fig. 2 shows examples of selected images recorded after sintering under different conditions. Fig. 2A corresponds to an image of a frit here produced, set on the Neubauer chamber and observed under the magnifier. In this case the polyimide coating was peeled off to obtain a clear view of the frit. Fig. 2B is an example of the normal appearance of a frit observed with the SEM. In few cases – *e.g.* Figure 2C – the sintered frits showed an aspect similar to powder or non-uniform little drops. It appeared occasionally and randomly distributed within the different conditions, and it was also observed in the images of frits sintered by other authors [10]. It would be attributed to fragmentation of particles by the fast change of temperature.

In a few instances layers of fully melted silica were found on the frit surface (*e.g.*, Fig. 2D and Fig. 2E). For example, in Fig. 2E the fused particles had begun to spill out into the surrounding space. The suspicion of contamination was ruled out by the results from spot analysis by EDS probe, showing a spectrum characteristic of silica – *i.e.*, prominent signals of both silicon and oxygen. These melted layers were randomly distributed among the different conditions and were also present in the SEM images of frits reported by other authors [8]. A solid layer such the shown in Fig. 2E but blocking the frit inlet, can seriously affect the efficiency of the porous device.

#### 3.2. Comparison between the DPM and the WPM

The evaluation of the DPM was based on the possible advantage of avoiding the evaporation step. Any capillary packed by means of the DPM has the particles dry and, consequently loose. Therefore, from the insertion of the capillary into the plaster bar until the placement of this set in the muffle oven the handling must be extremely careful in order to prevent the spilling and losing of the dry particles from both, the internal or external side of the bed. Nevertheless, occasionally the frits were formed further back, and the external surfaces did not match with the end surfaces of the capillaries, leaving an empty space as shown in Fig. 2F. In other instances, the frits were formed with a sloped surface such as illustrated in Fig. 2D, thus it is likely to produce band broadenings and reduction of the efficiencies.

Using the WPM and particles of 5  $\mu\text{m}$  on bare fused silica capillary tubes we did not experience problems of electrostatic charges during the introduction of particles: the use of a polar solvent prevented electrostatic repulsions, and also the introduction of a wet paste is easier. With the WPM the procedure resulted more robust and the packed bed of wet particles still remained immobilized after an incautious handling, even once the paste had dried.

A comparison of the packing methods in terms of success in the sintering procedure according to the definition given above show that frits produced by the DPM produce worst success rates. Fig. 3 shows the percentages of capillaries with frits sintered successfully using different conditions of temperature and exposure times. The left and right panels illustrate the results obtained with frits prepared with sintering beds packed by the DPM and the WPM, respectively. Clearly, the chances of getting successfully sintered frits are significantly greater by the WPM than by the DPM: indeed,

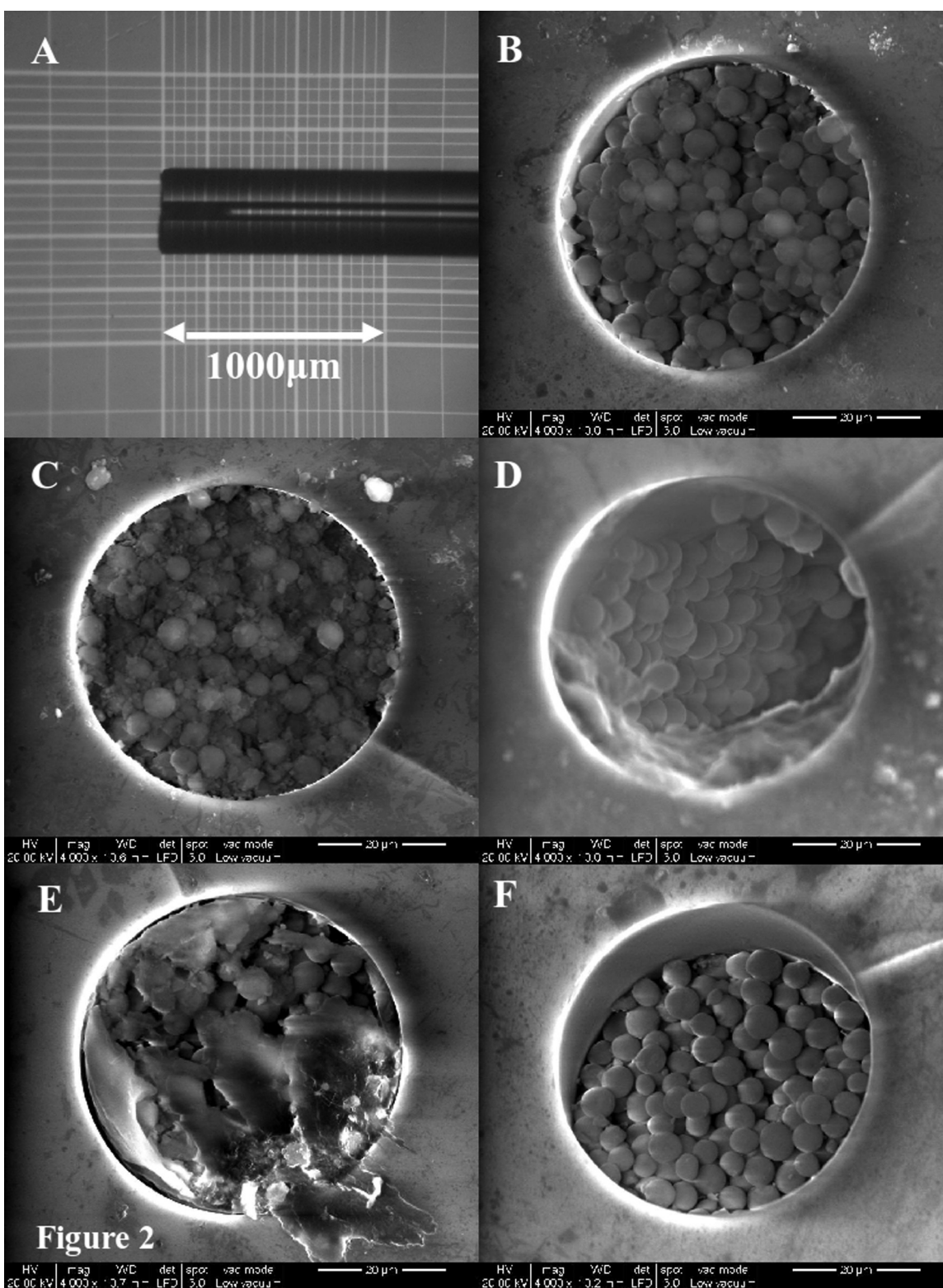


**Fig. 2.** A: Appearance of one of the shortest frits produced (300 μm) under magnification, with the polyimide coating intentionally removed. B: Surface of a frit produced by sintering a bed packed by the WPM. C: Front view of a frit sintered by the WPM where more fused and congealed particles were generated, giving a powder-like appearance. D: Front view of frit sintered by the DPM with a sloping surface after the loss of particles through inclination. E: Front view of a particular example of a frit with a part of the silica bed completely fused and spilled out. F: Front view of a frit based on the DPM sintered at a lower level because of the loss of particles.

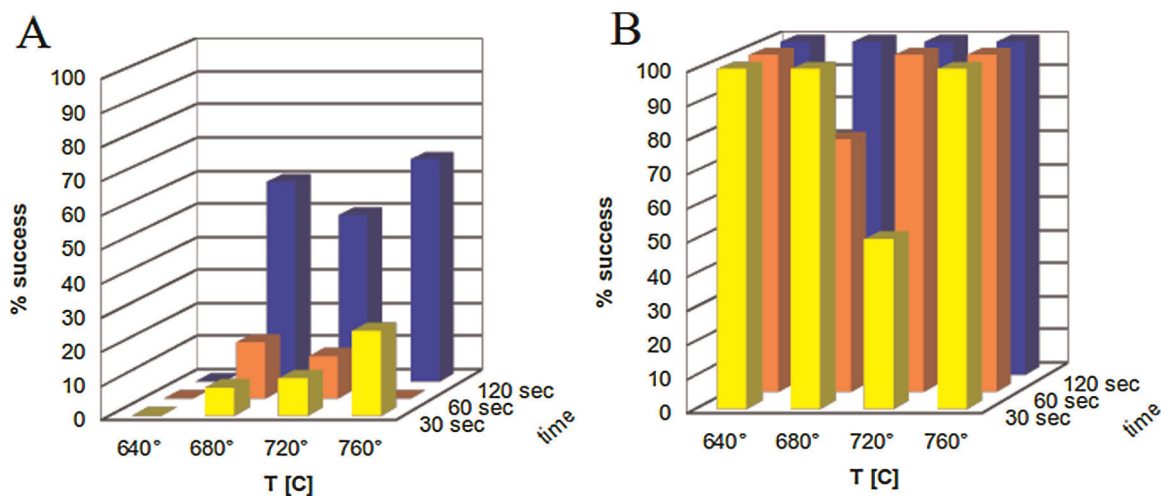


Fig. 3. Percent success in the sintering of particles under different conditions of temperature and exposure times with particles introduced by A (left panel): the DPM, and by B: (right panel) the WPM.

with the DPM we had success in fewer than half of the experiments. Even though the DPM showed a greater number of frits successfully formed at higher temperatures and longer times, the WPM showed success in almost all experiments, independently of the conditions.

In an attempt to improve the success rate in the generation of frits produced by the DPM, we replaced the particles of 5  $\mu\text{m}$  by those of 10  $\mu\text{m}$ , but the number of frits formed did not increase.

All of the foregoing observations and explanations lead to the conclusion that the WPM is the method to be recommended, and the following results presented here are accordingly based on only frits produced by means of the WPM.

When, after sintering, the capillaries were rinsed at 55–69 bar, more than 70% of the frits produced by sintering particles packed in this way withstood those pressures.

### 3.3. Frit lengths

After a removal of the loosen particles the frits produced by the proposed method could be measured. Panels A and B of Fig. 4 show with solid bars the averaged frit lengths obtained sintering under different conditions the particles introduced by the WPM. The standard deviations associated to each condition is indicated with vertical line on every bar.

Regardless of the used conditions, the average frit length resulted in all cases well below 1000  $\mu\text{m}$ , and in most of them below the 600  $\mu\text{m}$ . Frits of 600  $\mu\text{m}$  long are between 3 and 7 times shorter than those obtained following the classic method of radial heating – e.g., 2–4 mm [4,11,12].

As it is shown in Fig. 4A, longer exposition times do not increase significantly the mean length of sintered material, but also it increase the standard deviation.

Fig. 4B show the distribution of frit lengths as a function of the sintering temperatures. Intermediate temperatures, 640  $^{\circ}\text{C}$  and 720  $^{\circ}\text{C}$  produce shorter frits with smaller standard deviations.

### 3.4. Permeabilities and breaking pressures

The permeabilities have been calculated from the data of retention times of a dead-volume marker when eluted with a certain solvent flow by an applied constant pressure of 1000 mbar. Contributions owing to the frit and to the open tube should be taken into account. According to Poiseuille's law, valid for open tubes, the solvent linear velocity is:

$$u_0 = \frac{L_d}{t_0} = \frac{r^2 \Delta P}{8 \eta L_t} \quad (1)$$

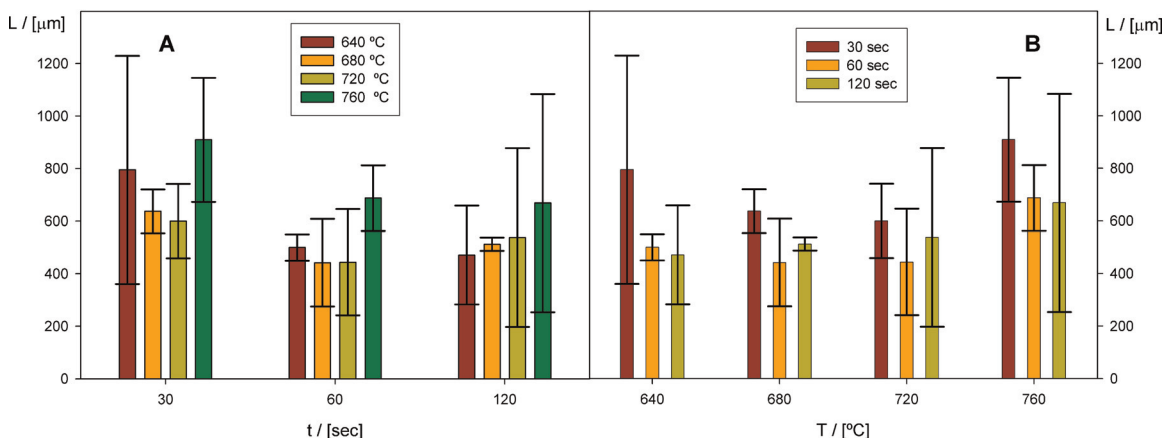


Fig. 4. A: Frit length vs. exposition time (sintering temperature of each bar is indicated in legend) and, B: frit length vs. temperature (exposition time of each bar is indicated in legend). Vertical slots are the s.d. of each bar

where  $u_0$  is the linear velocity of the solvent given as the effective length (*i.e.*, from the inlet to the detection window)  $L_d$ , over the elution time of the dead volume marker,  $t_0$ ;  $r$  the internal radius of the capillary tube;  $\Delta P$  the applied pressure;  $L_t$  the total length (from the inlet to the outlet); and  $\eta$  the solvent viscosity. In addition, velocities through porous media such as a sintered frit, can be obtained from Darcy's law:

$$u_0 = \frac{L_d}{t_0} = \frac{B\Delta P}{8\eta L_f} \quad (2)$$

where  $B$  is the permeability and  $L_f$  is the frit length.

An equation to obtain the permeability can be formulated by consideration that the total drop in pressure corresponds to the sum of the pressures from the resistance of both paths: the open capillary section and the contribution of the porous frit:

$$\Delta P = \frac{u_0 8\eta L_t}{r^2} + \frac{u_0 \eta L_f}{B\Delta P} \quad (3)$$

From this equation the permeability,  $B$ , can be obtained.

For the first determination of permeability, pure water was used as solvent, but the applied pressure was very frequently found to be insufficient to make the water flow through the frit. Flushes of pure methanol or methanol/water solutions, however, managed to reestablish flow through the frits immediately in all instances. Therefore, the determination of permeabilities was continued with 50% (v/v) methanol/water as the eluting solvent.

Since sintering conditions can affect permeability and resistance we measured these values as a function of the variables used in the sintering process. The objective was to find the safe zone for producing frits fulfilling the minimum required conditions. For this aim, capillaries with frits generated under each condition were used for the purposes of, firstly to measure the permeabilities and secondly, to determine its breaking pressures. Table 1 summarizes the results of these measurements averaging in each condition the results obtained in 2 or 3 frits. All the permeabilities had values higher than  $4 \times 10^{-11} \text{ cm}^{-2}$ .

Considering that a packed bed of porous silica particles of  $5 \mu\text{m}$  has a typical total porosity of 0.7, an calculation based on the modified Carman–Kozeny equation leads to an estimated value for the specific permeability of about  $3 \times 10^{-10} \text{ cm}^2$ . The general reduction of the permeabilities observed in our cases indicate that the sintering process produces a partial reduction of the interstitial porosity, from the typical value of 0.38 to a roughly 0.20–0.25.

The breaking pressures were higher than the minimum recommended, 55–69 bar, and some of the frits resisted pressures well above this limit. There is a certain proportional correlation between the breaking pressure and the frit length, and also an inverse correlation of the frit length with the breaking pressures.

These results were highly satisfying and indicated that practically all the frits generated under the different examined conditions fulfilled the requirements.

**Table 1**

Lengths, permeabilities, and breaking pressures of silica frits sintered under different conditions of temperature and exposure time.

| $T$ (°C) | $t$ (s) | $L$ ( $\mu\text{m}$ ) | $B$ ( $10^{11} \text{ cm}^{-2}$ ) | Breaking pressures (bar) |
|----------|---------|-----------------------|-----------------------------------|--------------------------|
| 640      | 120     | 688                   | 5.37                              | 224                      |
| 680      | 60      | 550                   | 42.5                              | 57                       |
| 720      | 30      | 500                   | 16.6                              | 52                       |
| 720      | 120     | 400                   | 5.64                              | 126                      |
| 760      | 60      | 750                   | 6.23                              | 176                      |
| 760      | 120     | 1050                  | 4.11                              | 252                      |

### 3.5. Generation of bubbles

Sintered end-frits often cause bubble formation when an electric field is applied through them. This problem constitutes a real challenge in CEC because bubbles produce a noisy baseline, plus an unstable current, or even a current breakdown; and once bubbles are formed inside the column, their elimination can prove to be difficult, especially in long columns where reasonable flows cannot be established by pressure, but only by electroosmosis. The theories about the origin of bubbles are controversial [13,14] and different authors have suggested to take different actions to prevent the formation of bubbles – *e.g.*, the use of (1) a high content of an organic solvent such as acetonitrile [15], (2) to use amine buffers such as 4-morpholineethanesulfonic acid (a.k.a. MOPS) or 3-(cyclohexylamino)-1-propanesulfonic acid (a.k.a. CAPS) [16], and (3) the use of degassed solutions; to pressurize the complete system; or to coat the surface of the sintered silica frit. Bartle et al. [7,17] however, found that the incidence of bubble formations is related directly to the length of the end frits and the applied voltage, and demonstrated that the occurrence is dramatically reduced when the frits are short (*i.e.*,  $<3 \text{ mm}$ ).

To evaluate the formation of bubbles in the frits generated by our method a specific voltage program was used under the most adverse experimental conditions – the latter being namely, (a) without surfactants, (b) with an inorganic buffer at pH values of high EOF (*e.g.*, borax buffer at pH 9.2), (c) with the lowest organic-solvent content usually admitted by the chromatographic stationary phases (here 10%, v/v of methanol), (d) using atmospheric pressure, (e) without degassing the solutions, and (f) without coating the silica frits. Three frits  $400 \mu\text{m}$ ,  $500 \mu\text{m}$ , and  $650 \mu\text{m}$  long were used. In order to apply the higher possible electric fields these capillaries were cut to the minimum length fitting the cassette of our instrument (*i.e.*,  $30 \text{ cm}$ ).

The program of voltage consisted in a first elevation of voltage, initially from 0 to 30 kV in 2 min and, then a drop back down to 0 kV after 2 min. Then, the voltage was elevated in a step to 30 kV and kept at this value for 20 min. The maximum electric field applied was  $100 \text{ V mm}^{-1}$ . This program was repeated in both, positive and negative polarities. The maximum currents obtained were between 80 and 90  $\mu\text{A}$ , positive and negative, respectively. No drops of the current were observed in our tests, and no sign of bubbles or increased noise appeared in the electropherogram baselines.

### 3.6. Band dispersion

A 50-cm-long capillary tube with a  $500\text{-}\mu\text{m}$  frit produced by sintering particles for 60 s at  $680^\circ\text{C}$  was used to test the degree of band dispersion associated with the frit. A second open capillary tube with the same dimensions was used as reference. The BGE injected was 5 mM borax in 10% (v/v) aqueous methanol in a solution of benzyl alcohol (*i.e.*, the EOF marker).

In order to isolate the band broadening associated with the sintered frit, the other contributions to dispersion must be subtracted. The subtraction of variances is valid, however, only when the contributions are the same in the tubes with and without a frit, and this condition did not obtain here. One of the additional contributions was the dispersion through diffusion because the EOF in tubes with or without frit is different and consequently, both the migration and the time-dispersal bands are different. Another contribution is the dispersion resulting from the injection volumes, a parameter that will differ in tubes with different flow resistances. The formulas to calculate these contributions to the dispersion in terms of the peak variances are as follows:

$$\sigma_t^2 = \sigma_{\text{inj}}^2 + \sigma_{\text{diff}}^2 + \sigma_{\text{frit}}^2 + \sigma_{\text{others}}^2 \quad (4)$$

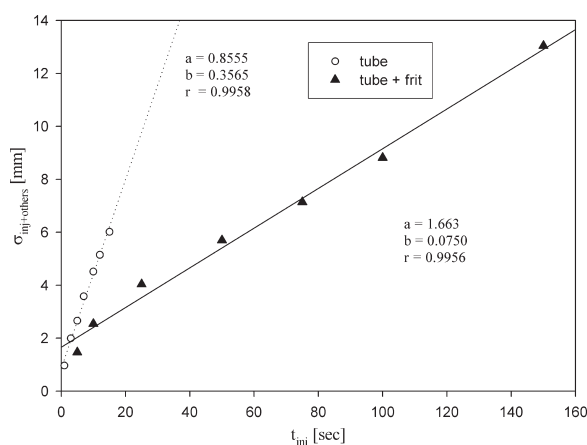


Fig. 5. Linear regression of peak standard deviations at different injection times in an open capillary tube and a capillary tube with a 500- $\mu\text{m}$  silica frit sintered by axial heating.

where  $\sigma_{\text{t}}^2$  refers to the total variance; while  $\sigma_{\text{inj}}^2$ ,  $\sigma_{\text{diff}}^2$ ,  $\sigma_{\text{frit}}^2$  and  $\sigma_{\text{others}}^2$  correspond to the variances associated with the injection volume, longitudinal diffusion, frit (if present), and other dispersions, respectively. In this treatment, we are assuming the approximation that the variance of other dispersions, grouped in the term  $\sigma_{\text{others}}^2$ , are equal in tubes with or without frits.

The diffusional dispersion was estimated by considering the Einstein–Smoluchowski equation:

$$\sigma_{\text{diff}}^2 = 2D_{\text{m}}t \quad (5)$$

where  $D_{\text{m}}$  is the diffusion coefficient and  $t$  corresponds to the migration time in seconds. We used a  $D_{\text{m}} = 1.0 \times 10^{-5} \text{ cm}^2 \text{ s}^{-1}$ , in which value corresponds to the diffusion coefficient of benzene in water at 25 °C, to estimate the variance resulting from longitudinal diffusion under each condition.

The dispersion of an ideal, and laminar flow injected volume can be calculated as:

$$\sigma_{\text{inj}} = \frac{V_{\text{inj}}}{\sqrt{12}} \quad (6)$$

where  $V_{\text{inj}}$  is the volume of the injection plug. An analysis with different injection volumes was carried out with each tube, upon injecting at 30 mbar during different times – between 1 and 15 s – in the tube without a frit, and at 50 mbar and between 5 and 150 s in the tube with the 500- $\mu\text{m}$  sintered frit. The experimental data indicated a linear relationship between  $\sigma_{\text{inj}}$  and  $t_{\text{inj}}$  for the peak profile obtained from both capillaries (Fig. 5). The regression coefficients and parameters are included in the same figure. The intercepts provided the standard deviations corresponding to zero injection volumes ( $\sigma_{\text{inj}}^2 = 0$ ) in both capillaries, whose variances were subtracted in Eq. (4) to calculate  $\sigma_{\text{frit}}^2$ . That difference between the two values gives  $\sigma_{\text{frit}}^2$  and its square root,  $\sigma_{\text{frit}} = 1.43 \text{ mm}$ . Upon consideration of the velocity of the band ( $v = 65.5 \text{ mm min}^{-1}$ ), the variance in minutes was estimated as  $\sigma_{\text{frit}}^2 = 0.000474 \text{ min}^2$ .

This dispersion value was obtained with benzyl alcohol and 10% (v/v) aqueous methanol as solvent and was run at voltages that gave migration times of around 380 s in a capillary tube with an uncoated

silica frit sintered by axial heating. In comparison, Dorsey et al. [4] measured values of around  $0.0007 \text{ min}^2$  for the migration times of benzene in pure acetonitrile of around 255 s in a capillary column with silica frits sintered by radial heating. As expected, the much shorter and homogeneous frits used here – most impressively – reduced the contribution from band broadening by about one-third.

#### 4. Conclusions

A new procedure to generate short silica frits at the ends of bare fused silica capillary tubes – based on the frontal exposure of the capillary tube with the silica particles inside to the heat of a muffle oven – is proposed and evaluated. The method produced notably short frits, from 3 to 7 times shorter than those usually obtained by radial heating, that proved also to be more efficient in terms of band broadening than frits produced by radial heating. Temperatures within the range 640–780 °C and exposure times from 30 to 120 s were systematically studied. The method was demonstrated to be robust and sufficiently flexible to enable the production of frits fulfilling the requirements of permeability, mechanical resistances and efficiencies for the preparation of capillary microcolumns compatible with electrodriven and also pressure driven capillary chromatographies.

#### Acknowledgements

This study was supported by CONICET (PIP-0777), ANPCyT (PICT2007-00316 and PICT-PRH2009-0038) and by Universidad Nacional de La Plata, Argentina. Dr. Donald F. Haggerty, a retired career investigator and native English speaker, edited the final version of the manuscript.

L. G. Gagliardi is grateful to Prof. E. Kennedler for his important contributions to our laboratory.

#### References

- [1] L.A. Colon, T.D. Maloney, A.M. Fermier, *Journal of Chromatography A* 887 (2000) 43.
- [2] N.W. Smith, M.B. Evans, *Chromatographia* 38 (1994) 649.
- [3] J.R. Chen, M.T. Dulay, R.N. Zare, F. Svec, E. Peters, *Analytical Chemistry* 72 (2000) 1224–1227.
- [4] S.M. Piraino, J.G. Dorsey, *Analytical Chemistry* 75 (2003) 4292.
- [5] B. Zhang, E.T. Bergström, D.M. Goodall, P. Myers, *Analytical Chemistry* 79 (2007) 9229.
- [6] F. Tan, S. Chen, Y. Zhang, Y. Cai, X. Qian, *Proteomics* 10 (2010) 1724.
- [7] R.A. Carney, M.M. Robson, K.D. Bartle, P. Myers, *Journal of High Resolution Chromatography* 22 (1999) 29.
- [8] R.J. Boughtflower, T. Underwood, C.J. Paterson, *Chromatographia* 40 (1995) 329.
- [9] R.T. Kennedy, J.W. Jorgenson, *Analytical Chemistry* 61 (1989) 1128.
- [10] B. Behnke, E. Grom, E. Bayer, *Journal of Chromatography A* 716 (1995) 207.
- [11] E.F. Hilder, C.W. Klampfl, M. Macka, P.H. Haddad, P. Myers, *Analyst* 125 (2000) 1.
- [12] Y.P. Zhang, Y.J. Zhang, W.J. Gong, N. Chen, A.I. Gopalan, K.P. Lee, *Microchemical Journal* 95 (2010) 67.
- [13] U. Pyell, *Journal of Chromatography A* 892 (2000) 257.
- [14] L.A. Colón, G. Burgos, T.D. Maloney, J.M. Cintrón, R.L. Rodríguez, *Electrophoresis* 21 (2000) 3956.
- [15] F. Lelievre, C. Yan, R.N. Zare, P. Gareil, *Journal of Chromatography A* 723 (1996) 145.
- [16] M.G. Cikalo, K.D. Bartle, M.M. Robson, P. Myers, M.R. Euerby, *Analyst* 123 (1998) 87R.
- [17] K.D. Bartle, R.A. Carney, A. Cavazza, M.G. Cikalo, P. Myers, M.M. Robson, S.C.P. Roulin, K. Sealey, *Journal of Chromatography A* 892 (2000) 279.